

Three-Dimensional Thermodynamic Analysis of Hydrogen- Rich Methanol Combustion Enhanced by Steam Reforming in a Finite-Time Framework[#]

Ruizhao Gao, Ruihua Chen^{*}, Kunteng Huang, Li Zhao^{*}

State Key Laboratory of Engines, Tianjin University, Tianjin 300072, China

(Corresponding Author: chenrh@tju.edu.cn, jons@tju.edu.cn)

ABSTRACT

Growing global concerns regarding carbon emissions and the demand for cleaner alternative energy sources have positioned methanol as a promising fuel for internal combustion engines, thanks to its hydrogen-rich composition, reduced carbon footprint, and favorable storage and transport properties. Nevertheless, methanol faces significant challenges in cold-start scenarios, largely due to its poor volatility and considerable heat absorption during evaporation. To tackle this issue, this research introduces a combined strategy integrating in-cylinder steam reforming of methanol with combustion enhanced by hydrogen enrichment. A finite-time thermodynamic framework was established to model the coupled combustion and reforming processes, taking into consideration critical variables including pressure ratio, air-fuel ratio, and rotational speed. Findings indicate that increased pressure ratio and air-fuel ratio contribute positively to engine performance, in contrast to engine speed, which shows a detrimental influence. Through multi-objective optimization, optimal operating parameters were identified as a pressure ratio of 20, an air-fuel ratio in the range of 13–15, and an engine speed between 1000 and 3000 rpm. This work aims to offer fundamental theoretical insights to guide and assist future endeavors in the design and refinement of methanol-fueled internal combustion engines.

Keywords: internal combustion engines, methanol steam reforming, finite-time thermodynamics, three-dimensional analysis

NONMENCLATURE

Abbreviations

| | |
|-----|------------------------|
| AFR | Air-fuel ratio |
| FT | Finite time |
| LHV | Low heating value |
| MD | Methanol decomposition |

| | |
|----------------|------------------------------------|
| MSR | Methanol steam reforming |
| PR | Pressure ratio |
| RPM | Revolutions per minute |
| WGS | Water-gas shift reaction |
| <i>Symbols</i> | |
| C_p | Specific heat at constant pressure |
| G | Gibbs free energy |
| H | Enthalpy |
| K | Equilibrium constant |
| k | Reaction rate constant |
| L | Piston stroke |
| m | Mass flow rate |
| n | Engine speed |
| P | Power |
| p | Pressure |
| Q | Heat |
| R | Ideal gas constant |
| r | Reaction rate |
| T | Temperature |
| v | Velocity |
| W | Work |
| η_{th} | Thermal efficiency |

1. INTRODUCTION

Against the backdrop of tightening emission regulations and growing environmental demands, developing clean alternative fuels for internal combustion engines has gained significant importance [1]. Methanol, with its low carbon content, high hydrogen content and favorable storage characteristics, emerges as a promising candidate, though its low volatility and high latent heat of vaporization present challenges for cold-start operation [2].

To address this, the integration of in-cylinder methanol steam reforming with combustion allows for real-time generation of hydrogen-enriched mixtures, which improves ignition stability under low-temperature conditions [3]. However, the reforming process is

[#] This is a paper for the 17th International Conference on Applied Energy (ICAE2025), December 8-12, 2025, Bangkok, Thailand.

dynamically coupled to engine operation, with parameters such as temperature, pressure, and residence time varying with engine speed—a relationship not adequately captured by conventional equilibrium thermodynamic models [4].

This study employs finite-time thermodynamic analysis to incorporate temporal and irreversible effects, evaluating the influence of engine speed on reforming completeness, hydrogen yield, and thermal efficiency. The results provide a theoretical basis for optimizing methanol-based engines with onboard hydrogen production.

2. METHODOLOGY

2.1 Cycle description

Fig. 1 and Fig. 2 illustrate the schematic diagram of an Otto cycle integrated with methanol steam reforming and its corresponding three-dimensional thermodynamic cycle representation, respectively. The axes represent temperature, entropy, and composition. During process 1-2, naturally aspirated fresh air is compressed to a state of high pressure and moderate temperature. In the latter stage of the compression stroke, methanol along with an appropriate amount of steam is injected into the cylinder. The liquid methanol is then heated and vaporized by the moderately warm air, and the gaseous methanol is progressively converted into hydrogen. At this stage, the fuel transitions from pure methanol to hydrogen-enriched methanol, denoted as process 2-2'. The cylinder now contains a mixture of hydrogen-enriched methanol and air. Subsequently, the hydrogen-enriched methanol is ignited by the spark plug. Its exothermic combustion produces high-temperature, high-pressure combustion products, primarily consisting of steam and carbon dioxide. Simultaneously, an excess of air remains in the cylinder, and following combustion, the contents comprise a mixture of combustion products and air. The combustion process of the hydrogen-enriched methanol and the associated changes in composition before and after combustion are depicted as process 2'-3. During the power stroke, the combustion products and excess air expand from state 3 to state 4, driving the piston and generating mechanical work output. After the power stroke, exhaust and intake strokes are performed sequentially. The concentration of combustion products gradually decreases, while that of fresh air increases, characterized by process 4-1. Thus, a complete internal combustion engine cycle incorporating methanol steam reforming is accomplished.

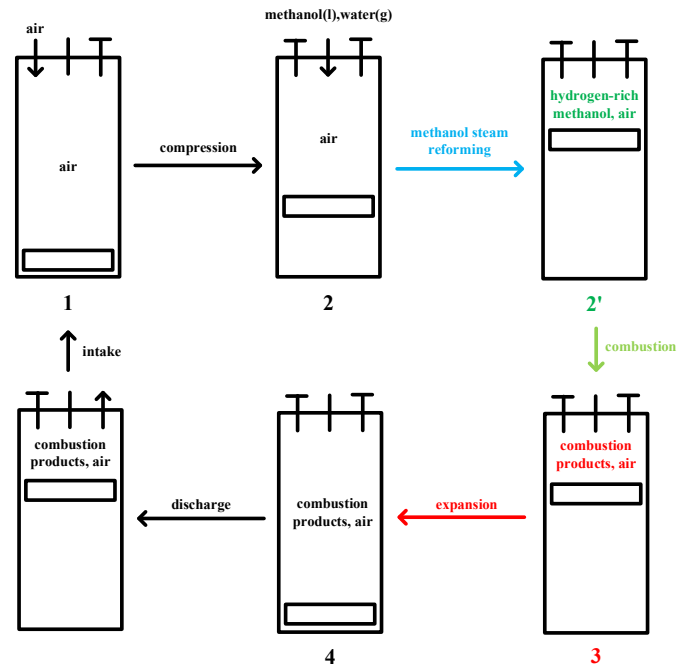


Fig. 1. The schematic diagram of an Otto cycle coupled with methanol steam reforming.

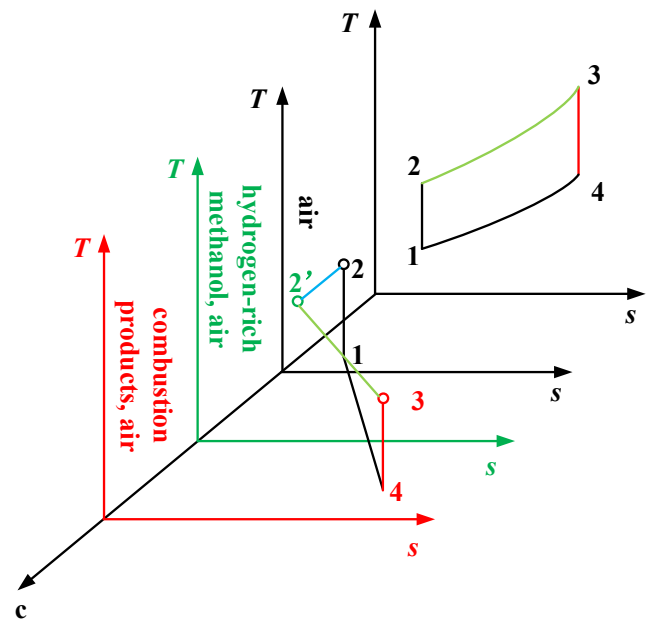


Fig. 2. The three-dimensional illustration of an Otto cycle coupled with methanol steam reforming.

2.2 Cycle model

This investigation is carried out under the following premises:

- (1) All thermodynamic phenomena are regarded as taking place in a steady-state regime;
- (2) The expansion and compression stages are modeled with defined isentropic efficiency parameters;

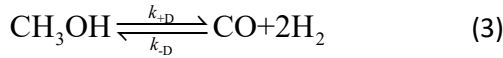
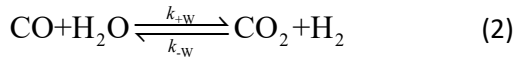
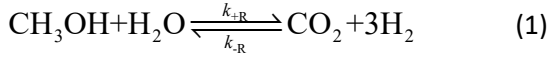
(3) Losses due to friction and viscous dissipation within the working medium are disregarded;

(4) The combustion chamber is treated as adiabatic, implying no thermal interaction between the system and the external environment;

(5) The ideal gas law is applied solely to the substances involved in the methanol steam reforming phase.

2.3 Kinetic model of methanol steam reforming

Due to the intricate nature of the reaction mechanisms involved in methanol reforming at the atomic scale, this study confines its analysis to the principal reactions that are universally unavoidable in most systems—specifically, steam reforming, the water-gas shift reaction, and methanol decomposition. The reaction equations are as follows:



And the kinetic model parameters are shown in the following table.

Table 1 Kinetic model parameters [5]

| Parameter | Value |
|---|---------------------------------------|
| Catalyst | Cu/ZnO/Al ₂ O ₃ |
| Composition | 10 : 5 : 85 |
| K _{OR} (m ² ·mol ⁻¹ ·s ⁻¹) | 4.07E+9 |
| K _{OD} (m ² ·mol ⁻¹ ·s ⁻¹) | 2.51E+17 |
| K _{OW} (m ² ·mol ⁻¹ ·s ⁻¹) | 2.31E+14 |
| E _R (J/mol) | 9.20E+4 |
| E _D (J/mol) | 8.25E+4 |
| E _W (J/mol) | 7.97E+4 |
| C _{S₁} ^T (mol/m ²) | 4.9E-8 |
| C _{S_{1a}} ^T (mol/m ²) | 1.4E-8 |
| C _{S₂} ^T (mol/m ²) | 5.7E-5 |
| C _{S_{2a}} ^T (mol/m ²) | 2.9E-8 |

The kinetic model used for methanol steam reforming (MSR), the water-gas shift reaction (WGS), and

methanol decomposition (MD) is described as follows [6]:

$$r_R = \frac{k_R K_{\text{CH}_3\text{O}}^* (p_{\text{CH}_3\text{OH}} / p_{\text{H}_2}^{1/2}) (1 - (p_{\text{H}_2}^3 p_{\text{CO}_2} / K_R p_{\text{CH}_3\text{OH}} p_{\text{H}_2\text{O}})) C_{\text{S}_1}^T C_{\text{S}_1a}^T}{(1 + K_{\text{CH}_3\text{O}}^* (p_{\text{CH}_3\text{OH}} / p_{\text{H}_2}^{1/2}) + K_{\text{HCOO}}^* p_{\text{CO}_2} p_{\text{H}_2}^{1/2} + K_{\text{OH}}^* (p_{\text{H}_2\text{O}} / p_{\text{H}_2}^{1/2})) (1 + K_{\text{H}^{(a)}}^{1/2} p_{\text{H}_2}^{1/2})} \quad (4)$$

$$r_W = \frac{k_W^* K_{\text{OH}}^* (p_{\text{CO}} p_{\text{H}_2\text{O}} / p_{\text{H}_2}^{1/2}) (1 - (p_{\text{H}_2} p_{\text{CO}_2} / K_W p_{\text{CO}} p_{\text{H}_2\text{O}})) C_{\text{S}_1}^T}{(1 + K_{\text{CH}_3\text{O}}^* (p_{\text{CH}_3\text{OH}} / p_{\text{H}_2}^{1/2}) + K_{\text{HCOO}}^* p_{\text{CO}_2} p_{\text{H}_2}^{1/2} + K_{\text{OH}}^* (p_{\text{H}_2\text{O}} / p_{\text{H}_2}^{1/2}))^2} \quad (5)$$

$$r_D = \frac{k_D K_{\text{CH}_3\text{O}(2)}^* (p_{\text{CH}_3\text{OH}} / p_{\text{H}_2}^{1/2}) (1 - (p_{\text{H}_2}^2 p_{\text{CO}} / K_D p_{\text{CH}_3\text{OH}})) C_{\text{S}_2}^T C_{\text{S}_2a}^T}{(1 + K_{\text{CH}_3\text{O}(2)}^* (p_{\text{CH}_3\text{OH}} / p_{\text{H}_2}^{1/2}) + K_{\text{OH}(2)}^* (p_{\text{H}_2\text{O}} / p_{\text{H}_2}^{1/2})) (1 + K_{\text{H}^{(2a)}}^{1/2} p_{\text{H}_2}^{1/2})} \quad (6)$$

The temperature dependences of each of these is given by Arrhenius and Vant hoff expressions. The values of equilibrium constants in rate expressions viz k_R , k_W , and k_D were calculated using the expressions:

$$-\ln(K) = \frac{\Delta G_0^\circ + \Delta H_0^\circ}{RT_0} + \frac{\Delta H_0^\circ}{RT} + \frac{1}{R} \int_{T_0}^T \frac{\Delta C_p^\circ}{T} dT - \int_{T_0}^T \frac{\Delta C_p^\circ}{R} dT \quad (7)$$

$$\int_{T_0}^T \frac{\Delta C_p^\circ}{R} dT = \Delta A \ln \tau + [\Delta B T_0 + (\Delta C T_0^2) (\frac{\tau+1}{2})] (\tau-1) \quad (8)$$

where

$$\tau = \frac{T}{T_0} \quad (9)$$

and $T_0 = 298$ K.

And the gas phase heat capacity is illustrated by Shomate equations:

$$C_p^\circ = A + B \times t + C \times t^2 + D \times t^3 + E / t^2 \quad (10)$$

$$H^\circ - H_{298.15}^\circ = A \times t + B \times t^2 / 2 + \quad (11)$$

$$C \times t^3 / 3 + D \times t^4 / 4 - E / t + F - H \quad (12)$$

$$S^\circ = A \ln t + B \times t + C \times t^2 / 2 + D \times t^3 / 3 - E / (2 \times t^2) + G \quad (13)$$

$$t = \frac{T}{1000}$$

The relative parameters are detailed in the NIST database NIST-JANAF Thermochemical Tables (Fourth Edition).

2.4 Finite time thermodynamic model

The heat released by the fuel can be calculated using the following formula:

$$Q_{\text{fuel}} = \sum_i m_i LHV_i \quad (14)$$

where i denotes the fuel components such as methanol, hydrogen, carbon monoxide, etc.

And the heat leakage is defined as [7]

$$Q_{\text{leak}} = B(T_2 + T_3 - 2T_0) \quad (15)$$

where B is a coefficient related to heat transfer.

The frictional loss due to piston movement is defined as [7]

$$P_{\mu} = \frac{dW_{\mu}}{dt} = 4\mu \frac{dX}{dt} \frac{dX}{dt} = 4\mu v^2 \quad (16)$$

$$\bar{v} = 2Ln \quad (17)$$

where L is piston stroke, n represents the engine speed.

And the net power output and thermal efficiency are

$$P_{\text{net}} = P_{\text{exp}} - P_{\text{com}} - P_{\mu} \quad (18)$$

$$\eta_{\text{th}} = \frac{P_{\text{net}}}{Q_{\text{fuel}} - Q_{\text{leak}}} \quad (19)$$

A Theory section should extend, not repeat, the background to the article already dealt with in the Introduction and lay the foundation for further work. In contrast, a Calculation section represents a practical development from a theoretical basis.

3. RESULTS AND DISCUSSIONS

3.1 Sensitivity analysis

Fig. 3 illustrates the influence of the pressure ratio on the hydrogen production. As shown, a higher pressure ratio positively affects methanol steam reforming. According to Le Chatelier's principle, an increase in pressure generally suppresses chemical reactions that result in a net increase in the total number of moles, which would theoretically impede methanol reforming for hydrogen production. However, simulation results indicate that the significant temperature rise induced by high pressure ratios substantially enhances the rate of the reforming reaction. This positive kinetic effect outweighs the inhibitory influence of pressure on reaction equilibrium, ultimately establishing a positive correlation between the pressure ratio and methanol steam reforming efficiency. This phenomenon suggests that, in methanol reforming-coupled systems, the promotion of reaction kinetics by pressure ratios plays a dominant role. Similarly, a higher air-fuel ratio promotes methanol reforming. Air, which barely participates in the methanol steam reforming reaction, can be regarded as an inert component. The introduction of inert components produces an effect similar to lowering the

reaction pressure, thus facilitating the reforming process.

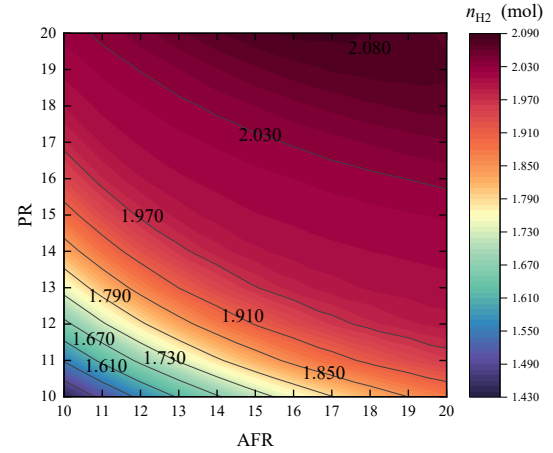


Fig. 3. The effect of the pressure ratio and air fuel ratio on hydrogen production.

Fig. 4 illustrate the effects of the pressure ratio and revolutions per minute on hydrogen production. As shown in Fig. 4, engine speed exerts a notable influence on system performance. Lower rotational speeds allow extended duration for the methanol steam reforming reaction, thereby promoting more complete conversion and enhancing hydrogen yield.

Fig. 5 presents the coupled influence of air-fuel ratio and engine speed on the finite-time thermal efficiency. The contours reveal a clear trade-off between chemical and mechanical efficiency under varying operating conditions.

Lower engine speeds (<1500 rpm) consistently yield higher thermal efficiencies across the air-fuel ratio range, with optimal performance observed near stoichiometric to slightly lean mixtures (AFR \approx 14–16). This behavior can be attributed to two complementary mechanisms: First, extended residence time at lower speeds allows more complete methanol reforming, enhancing hydrogen enrichment and promoting cleaner, more efficient combustion. Second, reduced piston velocities minimize frictional dissipation, preserving a larger portion of the indicated work as useful output.

As engine speed increases, thermal efficiency declines significantly, particularly under rich mixtures (AFR < 13). The efficiency loss stems from both kinetic and thermodynamic limitations: Shorter reaction time restricts reforming completeness, while increased heat transfer losses and higher friction power consumption reduce net work output. Notably, at high speeds (>2500 rpm), the system shows greater sensitivity to air-fuel ratio variations, with leaner mixtures (AFR > 16)

exhibiting steeper efficiency degradation due to excessive charge dilution and slower combustion rates.

The optimal operating window emerges at moderate speeds (1000–2000 rpm) with slightly lean mixtures (AFR \approx 14–15), where the benefits of sufficient reforming time and acceptable friction losses are balanced.

In summary, system performance results from the coupling of multiple parameters: engine speed affects reforming completeness and thermal efficiency through reaction duration and mechanical losses; the air-fuel ratio requires balancing between combustion and reforming processes; while the pressure ratio mainly governs the thermal driving force for reforming. Practical optimization should therefore consider the interactions among these parameters to achieve synergistic improvements in both hydrogen production and thermal efficiency.

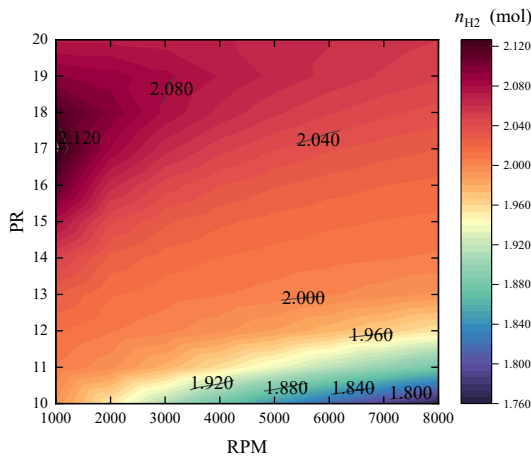


Fig. 4. The effect of the pressure ratio and revolutions per minute on hydrogen production.

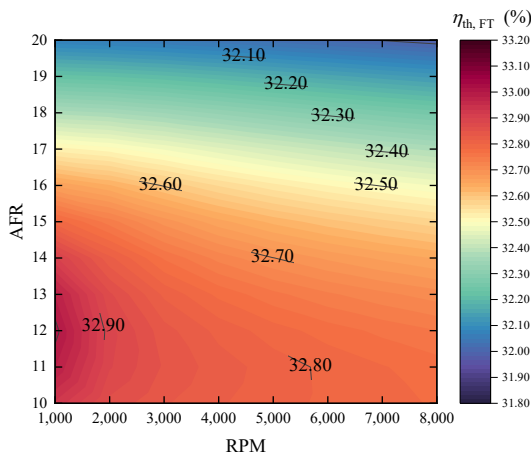


Fig. 5. The effect of the air fuel ratio and engine speed on finite time thermal efficiency.

3.2 Comparison between equilibrium model and finite time model

The comparison between equilibrium thermal efficiency and finite-time thermal efficiency is displayed as Fig. 6. The comparison between equilibrium thermal efficiency and finite-time thermal efficiency reveals critical insights into the practical performance limits of the methanol steam reforming integrated Otto cycle.

The finite-time thermal efficiency consistently lies below the equilibrium value across all operating conditions, with the deviation widening under higher engine speeds and richer mixtures.

At lower speeds, the efficiency deficit is primarily attributable to incomplete methanol reforming and limited hydrogen yield, as the available reaction time remains insufficient to reach chemical equilibrium. As speed increases, frictional dissipation becomes progressively more dominant.

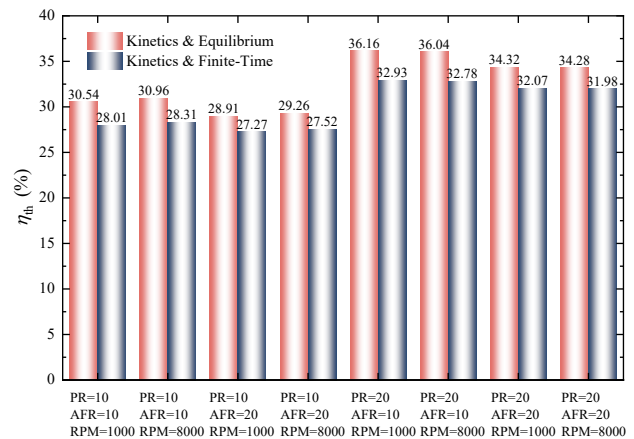


Fig. 6. The comparison between equilibrium thermal efficiency and finite time thermal efficiency.

3.3 Dual-objective optimization

As illustrated in Fig. 7, the dual-objective optimization of the integrated methanol steam reforming Otto cycle has identified two distinct operating points, each optimized for a different weighting ratio between hydrogen production and thermal efficiency.

Under balanced optimization weighting (0.5/0.5) with PR = 19.99, AFR = 12.69, and RPM = 1386.58, the system achieves a hydrogen production rate of 2.07 mol and a finite-time thermal efficiency of 32.62%. The lower speed allows extended reaction time for more complete methanol reforming, while the rich mixture supports higher hydrogen yield, though at the cost of slightly lower combustion efficiency. At a weighting ratio of 0.6/0.4 favoring hydrogen production, operating under PR = 19.99, AFR = 15.91, and RPM = 3000.00 results in a hydrogen yield of 2.10 mol with a corresponding finite-time thermal efficiency of 32.60%. This case

demonstrates that higher engine speed combined with a leaner mixture can maintain comparable hydrogen production while slightly improving thermal efficiency. The lean mixture enhances combustion completeness and reduces thermal losses, partially compensating for the kinetic limitations imposed by shorter reaction time at high RPM. The lean mixture enhances combustion completeness and reduces thermal losses, partially compensating for the kinetic limitations imposed by shorter reaction time at high RPM.

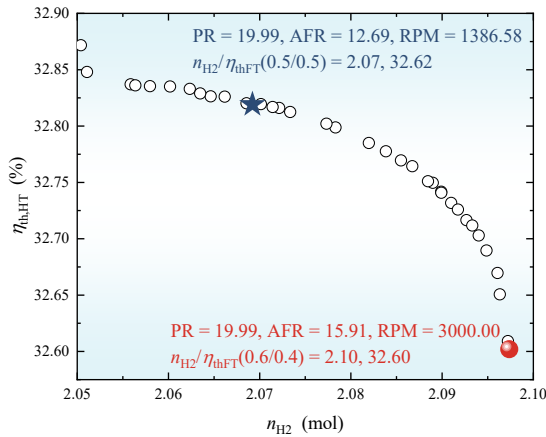


Fig. 7. The comparison between equilibrium thermal efficiency and finite time thermal efficiency.

4. CONCLUSIONS

This paper investigates a novel methanol internal combustion engine cycle integrated with methanol steam reforming. A comprehensive finite time thermodynamic performance evaluation of the proposed cycle is conducted. In addition, both sensitivity analysis and dual-objective optimizations are carried out to enhance cycle performance. The main conclusions of this study are summarized as follows:

- (1) Hydrogen production increases by approximately 1.6% and 0.35% per unit rise in pressure ratio and air-fuel ratio, respectively, but decreases by about 1% per 1000-rpm increase in rotational speed.
- (2) Incorporating methanol steam reforming kinetics results in an Otto cycle efficiency that is 1.5-3% lower under finite-time thermodynamics compared to the equilibrium assumption.
- (3) The equilibrium thermal efficiency and finite-time thermal efficiency reach their highest level at a pressure ratio of 20 and a rotational speed of 1000 rpm, with corresponding air-fuel ratios of 10 and 12 respectively.
- (4) Optimizing for hydrogen production and thermal efficiency together—with a pressure ratio of 20,

an air-fuel ratio between 13 and 15, and a rotational speed of 1000-3000 rpm—delivers balanced performance in both objectives.

ACKNOWLEDGEMENT

The authors gratefully acknowledge the support funded by the National Key R&D Program of China (No. SQ2025YFE0199400).

REFERENCE

- [1] Rao X., Yuan C., Guo Z., Xu Y., Sheng C. Methanol as an alternative fuel for marine engines: A comprehensive review of current state, opportunities, and challenges. *Renewable Energy* 2025;252:123562. <https://doi.org/10.1016/j.renene.2025.123562>.
- [2] Osman A.I., Nasr M., Lichtfouse E., Farghali M., Rooney D.W. Hydrogen, ammonia and methanol for marine transportation. *Environmental Chemistry Letters* 2024;22:2151-8. <https://doi.org/10.1007/s10311-024-01757-9>.
- [3] Tartakovsky L., Sheintuch M. Fuel reforming in internal combustion engines. *Progress in Energy and Combustion Science* 2018;67:88-114. <https://doi.org/10.1016/j.pecs.2018.02.003>.
- [4] Gao R., Huang K., Chen R., Zhao R., Li J., Shen J., et al. Three-dimensional thermodynamic analysis of hydrogen-enriched methanol combustion enabled by integrated steam reforming. *Energy* 2025;337:138625. <https://doi.org/10.1016/j.energy.2025.138625>.
- [5] Agarwal V., Patel S., Pant K.K. H2 production by steam reforming of methanol over Cu/ZnO/Al2O3 catalysts: transient deactivation kinetics modeling. *Applied Catalysis A: General* 2005;279:155-64. <https://doi.org/10.1016/j.apcata.2004.10.026>.
- [6] Asprey S.P., Wojciechowski B., Peppley B.A. Kinetic studies using temperature-scanning: the steam-reforming of methanol. *Applied Catalysis A: General* 1999;179:51-70. [https://doi.org/10.1016/S0926-860X\(98\)00300-7](https://doi.org/10.1016/S0926-860X(98)00300-7).
- [7] Ge Y., Chen L., Sun F. Finite-time thermodynamic modelling and analysis of an irreversible Otto-cycle. *Applied Energy* 2008;85:618-24. <https://doi.org/10.1016/j.apenergy.2007.09.008>.